

## ARTICLES

**A Statistical Kinetic Model for the Bulk Degradation of PLA-*b*-PEG-*b*-PLA Hydrogel Networks: Incorporating Network Non-Idealities****Andrew T. Metters,<sup>†</sup> Kristi S. Anseth,<sup>†,‡</sup> and Christopher N. Bowman<sup>\*,†,§</sup>***Department of Chemical Engineering, University of Colorado, Boulder, Colorado 80309-0424, Howard Hughes Medical Institute, 4000 Jones Bridge Road, Chevy Chase, Maryland 20815-6789, and Department of Restorative Dentistry, University of Colorado Health Sciences Center, Denver, Colorado**Received: November 7, 2000; In Final Form: April 30, 2001*

Experimental studies and theoretical predictions of the bulk-degradation behavior of nonideal PLA-*b*-PEG-*b*-PLA hydrogels were performed. The theoretical predictions are based on a previously developed model to which refinements have been made, including the incorporation of a more realistic description of the cross-linked, copolymer network structure. Also, structural complexities such as unreacted vinyl groups, multiple degradation sites along the polymer chains, and distributions in the degrees of polymerization of the cross-links, cycles, and backbone chains that comprise the network are now included in the model. Each of these factors has a dramatic effect on the bulk-degradation behavior of the hydrogels, and this second generation model incorporates these factors into the theoretical description of the experimental system with only a minimal increase in the number of parameters and complexity of the model equations.

**Introduction**

The PLA-*b*-PEG-*b*-PLA hydrogels first described by Sawhney et al.<sup>1</sup> are water swellable, cross-linked networks. More unique, the cross-links within these networks, because they contain PLA units, are cleaved systematically in the presence of water. Applications for these degradable, cross-linked networks include improved drug delivery devices, tissue adhesives, orthopedic implants, and adhesion barriers.<sup>2–5</sup> Previously, a theoretical model to predict the bulk-degradation behavior of these hydrogels was developed.<sup>6</sup> This modeling methodology combines kinetic parameters pertaining to the hydrolysis of degradable units within the copolymer with structural details of the cross-linked networks. Utilizing such an approach, the model accounts for the continuously changing network structure during degradation and can accurately predict the complex erosion profiles from the cross-linked hydrogels. Such predictable and controllable degradation behavior is necessary to tailor these materials effectively for a given application.

Although the previously developed model can successfully predict the degradation behavior of a limited number of hydrogel networks formed under well-controlled conditions, its simplified approach assumes many idealities and does not provide an accurate physical representation of most polymer networks formed experimentally.<sup>6</sup> Numerous additional chemical and structural complexities must be considered if the theoretical description is to capture the subtle differences in the complex

degradation process of these nonideal hydrogels. Only with this more detailed approach can the degradation of gels produced under a wide range of conditions and with a variety of monomers be predicted accurately.

One important physical characteristic that must be incorporated into the previous modeling scheme is the presence of partially reacted PLA-*b*-PEG-*b*-PLA segments. In the ideal network structure described in an earlier paper,<sup>6</sup> both ends of the macromer were assumed to be 100% functionalized with acrylate groups during synthesis and fully reacted via cross-linking or cyclization into the network during polymerization. However, in reality, a significant number of unreacted macromer chain ends are present in the experimental hydrogel networks due to either incomplete functionalization during macromer synthesis or incomplete acrylate polymerization.

Another nonideality of real hydrogel networks is the presence of multiple degradation sites within the PLA blocks. Each lactic acid repeat unit within a PLA block contains a hydrolytically labile ester bond. The original model followed only the degradation kinetics of entire PLA blocks, not individual ester bonds. Redefining the degradation behavior of the PLA-*b*-PEG-*b*-PLA hydrogels based on the number, location, and distribution of individual ester bonds within the network allows one to predict quantitative differences in the degradation behavior of various PLA-*b*-PEG-*b*-PLA systems.

Distributions in the number of repeat units making up the cross-links, cycles, and backbone chains of the network cannot be avoided during macromer synthesis and subsequent polymerization. The influence of these distributions, as well as the other characteristics described above, on the overall degradation behavior of the PLA-*b*-PEG-*b*-PLA hydrogels is examined here. In this work, the previously developed theoretical model is

\* To whom correspondence should be addressed. E-mail: Christopher.Bowman@Colorado.edu. Fax #: (303) 492-4341

<sup>†</sup> Department of Chemical Engineering, University of Colorado.

<sup>‡</sup> Howard Hughes Medical Institute.

<sup>§</sup> Department of Restorative Dentistry, University of Colorado Health Sciences Center.

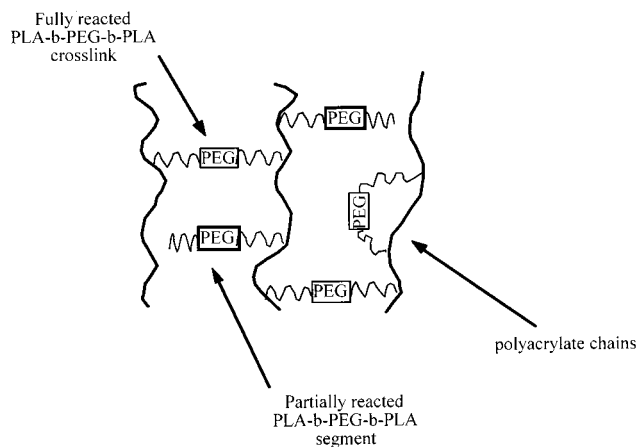


**Figure 1.** Cross-linked PLA-*b*-PEG-*b*-PLA hydrogel structure illustrating the presence of partially reacted PLA-*b*-PEG-*b*-PLA segments through either incomplete functionalization or polymerization.

extended to predict more accurately the bulk-degradation behavior of real hydrogel networks through the addition of a minimal number of parameters to account for network nonidealities.

### Materials and Methods

The PLA-*b*-PEG-*b*-PLA macromers used in this study were synthesized according to the techniques first described by Sawhney et al.<sup>1</sup> and as described in a previous paper.<sup>7</sup> Briefly, the macromers were synthesized in a two-step process. In the first step, the dihydroxy poly(ethylene glycol) (PEG) was reacted with D,L-lactide for 6 h at 135 °C under an argon atmosphere using stannous octoate as a catalyst. This intermediate block copolymer was then prepared by dissolving in methylene chloride, precipitating in diethyl ether, vacuum filtering, and then drying under vacuum. In the second step, the chain ends of the copolymer were acrylated after dissolving the polymer once again in methylene chloride and adding a 3-fold excess of triethylamine and acryloyl chloride. The solution was then reacted under an argon atmosphere at 0 °C for 12 h and then at room temperature for another 12 h. A second precipitation in diethyl ether followed by vacuum filtration produced a fluffy, white powder. All chemicals used in the synthesis were obtained from Aldrich, except for the D,L-lactide which was purchased from Polysciences. <sup>1</sup>H NMR spectroscopy (Varian VSR-500S) of the products in d-CHCl<sub>3</sub> was used to quantitatively characterize the structures of the acrylated copolymers.

The notation given for the synthesized PLA-*b*-PEG-*b*-PLA macromers refers to the molecular weight of the PEG chain followed by the symmetrical number of lactide repeat units on each end. For example, 4600-5 refers to a macromer containing a 4600 Da PEG chain with an average of five lactide repeat units on either side. The ends of this copolymer chain are then capped to varying degrees with acrylate functionalities to allow photopolymerization and cross-linking of the chains into a system similar to the network illustrated in Figure 1.

Photopolymerization of the macromers was initiated with a 365 nm light source (Blak-Ray model B100 AP) with a peak intensity of approximately 15 mW/cm<sup>2</sup>. The solid macromer was dissolved in deionized water to a specified concentration. A 20 wt % solution of the photoinitiator 2,2-dimethoxy-2-phenylacetophenone (Irgacure 651, Ciba Geigy) in ethanol was then added to the macromer solution until the initiator concentration was 0.2 wt %. Photopolymerization of the final mixture

produced hydrogel disks approximately 1.0 cm in diameter and 1.0 mm thick.

Degradation studies were conducted in a 7.4 pH phosphate buffered solution (PBS, Fisher) at 37 °C. At specific time points, swelling and mass-loss measurements were taken. To obtain the volumetric swelling ratio of the gels ( $Q$ ), a disk was removed and weighed in air ( $W_{A,S}$ ) and in heptane ( $W_{h,S}$ ). The polymer weight ( $W_{A,D}$ ) was obtained by drying the sample under vacuum until constant weight.  $Q$  was then calculated according to eq 1

$$Q = \frac{(W_{A,S} - W_{h,S})/\rho_h}{W_{A,D}/\rho_p} \quad (1)$$

where  $\rho_h$  is the density of heptane (0.684 g/mL) and  $\rho_p$  is the density of the dried polymer (assumed to be 1.1 g/mL). Percent mass loss from the sample was determined according to the procedure previously described.<sup>7</sup>

### Results and Discussion

**Original Model Development.** As described in the first paper of this series, the theoretical model accounts for mass loss by calculating the probability that a certain species is “released” from the cross-linked gel. Neglecting lactic acid residues, there are three primary erosion products: (1) pure PEG chains, (2) pure polyacrylate chains, and (3) polyacrylate chains with a fraction of partially degraded PLA-*b*-PEG-*b*-PLA segments still attached.<sup>6</sup> The polyacrylate chains, also referred to as the kinetic chains of the network, are formed through the radical polymerization of the acrylate end groups. As derived in the original paper, the mass loss due to these three products can be related to the fraction of PLA segments hydrolyzed ( $P$ ) through a series of mathematical equations<sup>6</sup>

$$F_{PA} = [1 - (1 - P)^2]^N \quad (2)$$

$$F_{PEG} = P^2 + F_{PA}P(1 - P) \quad (3)$$

$$\% \text{ mass loss} = (W_{PA}F_{PA} + W_{PEG}F_{PEG}) \quad (4)$$

Here, the fractions of polyacrylate kinetic chains ( $F_{PA}$ ) and PLA-*b*-PEG-*b*-PLA segments ( $F_{PEG}$ ) that are released from the network at a given time during the degradation depend on the fraction of hydrolyzed PLA segments ( $P$ ) and the number of cross-links originally attached to each kinetic chain ( $N$ ). These two fractions are then weighted by their corresponding network mass percents ( $W_{PA}$  and  $W_{PEG}$ ) to calculate the total percent mass loss from the degrading network. The fraction of hydrolyzed PLA blocks within the degrading cross-linked gel ( $P$ ) is calculated using a pseudo first-order kinetic equation

$$P = 1 - \left( \frac{n_{PLA}}{n_{PLA}^o} \right) = 1 - e^{-k't} \quad (5)$$

where  $n_{PLA}$  and  $n_{PLA}^o$  are the current and original number of undegraded PLA blocks within the network, respectively, and  $k'$  is the pseudo first-order reaction rate constant for the hydrolysis of the entire PLA block. By incorporating this kinetic dependence into the structural equations, the overall network mass loss of the network as a fraction of degradation time ( $t$ ) can be determined.

Because of the high degree of swelling exhibited by the PLA-*b*-PEG-*b*-PLA gels when placed in an aqueous environment, a number of assumptions are still necessary to simplify the mass-loss model. The hydrolysis of the PLA blocks is assumed to

occur homogeneously throughout the hydrophilic network with no crystalline regions present. The presence of amorphous vs crystalline PLA within the network will depend on three primary factors: the weight fraction of ethylene glycol vs lactic acid, the type of lactide used to form the PLA (D, L, or D, L), and the storage conditions of the gel. As long as the gel consists predominantly of PEG and the gels are not allowed to deswell significantly before the degradation experiments, no crystallization of PLA will occur. All gels used in the present study contain an order of magnitude greater number of ethylene glycol repeat units compared to lactic acid repeat units and are always kept in their swollen state, thereby maintaining an amorphous, homogeneous network.

Pseudo first-order reaction kinetics are also assumed because of the high water content and low acid-species concentrations that are generally present in hydrogels of this type,<sup>7,8</sup> although higher order and more complex kinetic mechanisms can be readily incorporated to describe more complicated cross-link degradation processes.

Finally, diffusion of degradation products out of the highly swollen network is assumed to occur much faster than the degradation. Therefore, once a species is released from the theoretically described network, the mass of this erosion product immediately appears as a loss in the mass of the overall network. This assumption is easily verified for the corresponding experimental systems by comparing the experimentally measured time scales for first-order degradation ( $1/k'$ , where  $k'$  is the first-order hydrolysis rate constant) and solute diffusion ( $L^2/D$ , where  $L$  is the diffusion path length and  $D$  the diffusion coefficient). The predominant degradation products in these gels, especially at early times, are PEG chains with molecular weights of  $10^3$ – $10^4$  Da. Estimates for their diffusion coefficients in highly swollen networks can be found in the literature and are on the order of  $10^{-5}$ – $10^{-4}$  mm<sup>2</sup>/s.<sup>9,10,11</sup> Combining these values with information about the geometry of the polymerized disks ( $L = 0.5$  mm) yields diffusion time scales for the degradation products on the order of a few hours. The first-order degradation rate constants observed for the same networks, however, are on the order of  $10^{-5}$ – $10^{-4}$  min<sup>-1</sup>, generating much longer degradation time scales on the order of days.<sup>6,7,12</sup>

In addition to the theoretical validation, a series of partial-degradation experiments were performed to measure the effect, if any, of degradation products on the degradation rate. In these experiments, gels were removed from the degradation media at specified times, swollen in organic solvent to remove any soluble fraction (including any degradation products), and then returned to the buffer solution. Upon their return these gels showed the same behavior as undisturbed gels with no change in degradation kinetics, indicating that the degradation products had no effect on degradation rate.<sup>12</sup>

**Model Refinement: Partially Reacted PLA-*b*-PEG-*b*-PLA Segments.** The original model of the network structure only considered fully reacted, divinyl PLA-*b*-PEG-*b*-PLA macromers. Upon complete reaction, these macromers formed either cycles or cross-links within the cross-linked network structure. Realistically, two other species are present after polymerization of these systems: macromers with only one double bond reacted and macromers with neither double bond reacted. These species will be present due to either incomplete functionalization during the macromer synthesis, i.e., incomplete acrylation of the terminal alcohol functionalities, or incomplete acrylate reaction during polymerization. Therefore, prior to degradation, the cross-linked network may more closely resemble the structure shown in Figure 1.

Completely unreacted macromers do not contribute to the network structure and will simply be part of the sol fraction. Therefore, this moiety is not considered in the network mass-loss equations. The presence of partially reacted macromers, however, must be accounted for in the bulk-degradation model to provide accurate mass-loss predictions. This network imperfection was incorporated into the theoretical model by including additional terms in the original mass-loss equations (eqs 2–4). Partially reacted macromers are those PLA-*b*-PEG-*b*-PLA segments attached to the surrounding network through reaction of only one vinyl group. These segments are then released from the network when the single PLA unit next to the reacted vinyl group is hydrolyzed. Release of fully reacted segments require both PLA linkages to be cleaved. To account for both types of mass loss, the first term on the right-hand side of eq 3 ( $P^2$ ) was replaced by

$$F_{\text{PEG}_1} = x_1P + x_2P^2 \quad (6)$$

Here,  $x_1$  and  $x_2$  are the fractions of PLA-*b*-PEG-*b*-PLA segments singly and doubly reacted into the network, respectively.

Because singly reacted PLA-*b*-PEG-*b*-PLA segments can arise from incomplete functionalization or polymerization, both of these processes were involved in calculating the fractions of singly,  $x_1$ , and doubly reacted,  $x_2$ , macromer

$$x_2 = ZX \quad (7)$$

$$x_1 = (1 - x_2) = (1 - ZX) \quad (8)$$

where  $Z$  is the fraction of macromer chain-ends functionalized, and  $X$  is the double bond conversion after polymerization. The above equations for  $x_1$  and  $x_2$  assume a statistical distribution for the acrylate functionalization and also assume the reactivity of one acrylate chain end to be completely independent of the other. The double bond conversion,  $X$ , can be obtained using analytical methods such as Fourier Transform Infrared Spectroscopy (FTIR) or Differential-Scanning Calorimetry (DSC) to monitor the polymerization kinetics, whereas the fraction of macromer chain-ends functionalized,  $Z$ , can be calculated from <sup>1</sup>H NMR analysis of the initial macromer.

With the description that this more realistic model provides, all PLA-*b*-PEG-*b*-PLA segments do not form cross-links when  $Z < 1$ , even when 100% conversion is reached and there is no cyclization. Therefore, a distinction must be made between the number of cross-links originally attached to each kinetic chain ( $N$ ) and the total kinetic chain length ( $L$ ). Using the parameters defined above, the relationship between these two parameters is

$$N = x_2(1 - f_c)L = ZX(1 - f_c)L \quad (9)$$

Here,  $f_c$  is the fraction of diacrylated PLA-*b*-PEG-*b*-PLA segments that form cycles rather than cross-links. Using eq 9, the fraction of polyacrylate chains that can be released from the network at any point during the degradation process ( $F_{\text{PA}}$ ) is now rewritten from eq 2 as

$$F_{\text{PA}} = [1 - (1 - P)^2]^{ZX(1 - f_c)L} \quad (10)$$

Equation 5 gives the fraction of PLA-*b*-PEG-*b*-PLA segments that can be released individually from the cross-linked network as a function of degradation. However, the PLA-*b*-PEG-*b*-PLA segments that release while attached to a polyacrylate chain ( $F_{\text{PEG}_2}$ ) must also be accounted for by rewriting the second term

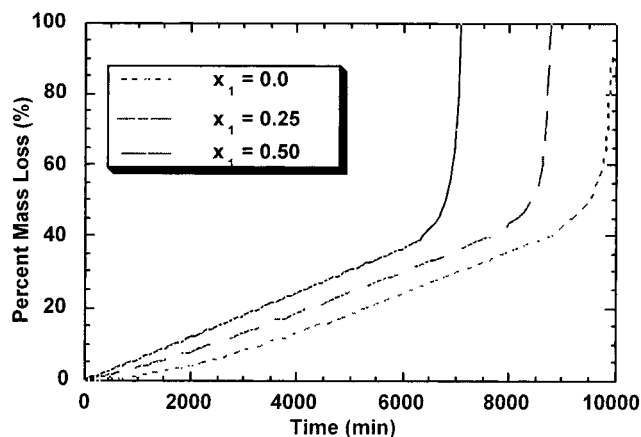


**Figure 2.** Predicted mass loss vs degradation time for hydrogels with a constant kinetic chain length ( $L = 20$ ) and increasing fraction of singly reacted PLA-*b*-PEG-*b*-PLA segments ( $x_1 = 0.0, 0.25, 0.50$ ). Model parameters:  $W_{\text{PEG}} = 0.95, f_c = 0.0$ , and  $k' = 1.2 \times 10^{-4} \text{ min}^{-1}$ .

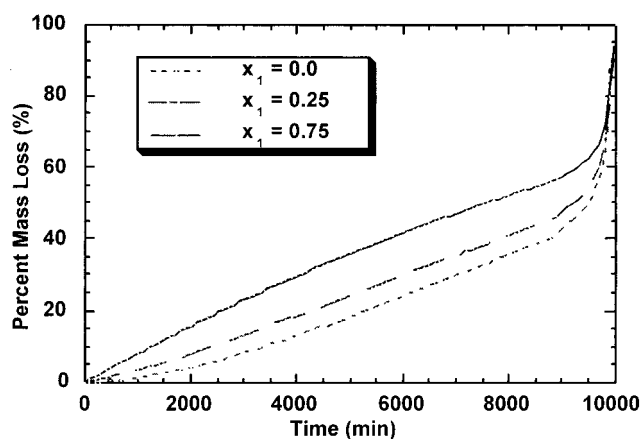


**Figure 3.** Predicted mass loss vs degradation time for hydrogels with a constant number of cross-links per chain ( $N = 20$ ) and increasing fraction of singly reacted PLA-*b*-PEG-*b*-PLA segments ( $x_1 = 0.0, 0.25, 0.75$ ). Model parameters:  $W_{\text{PEG}} = 0.95, f_c = 0.0$ , and  $k' = 1.2 \times 10^{-4} \text{ min}^{-1}$ .

of eq 3. Accounting for both singly and doubly reacted PLA-*b*-PEG-*b*-PLA segments, the second term of eq 3 is modified to give

$$F_{\text{PEG}_2} = F_{\text{PA}}[(1 - f_c)[x_1(1 - P) + x_2P(1 - P)] + f_c x_2(1 - P^2)] \quad (11)$$

The two mechanisms that contribute to the release of PLA-*b*-PEG-*b*-PLA segments are then added together

$$F_{\text{PEG}} = F_{\text{PEG}_1} + F_{\text{PEG}_2} \quad (12)$$

and the final calculation of mass loss from the degrading hydrogel proceeds according to eq 4, as before, but with newly defined terms. It should be mentioned that the final breakdown of the network due to a mechanism termed “reverse gelation” depends only on two parameters, the fraction of hydrolyzed PLA units ( $P$ ) and the original number of cross-links per kinetic chain ( $N$ ). Thus, the onset of reverse gelation will be predicted exactly as described for the ideal network.<sup>6,13</sup>

The dependence of mass-loss predictions on various model parameters is shown in Figures 2 and 3. Figure 2 shows the mass loss predictions from a series of hydrogels with constant kinetic chain lengths ( $L$ ) but increasing fractions of singly

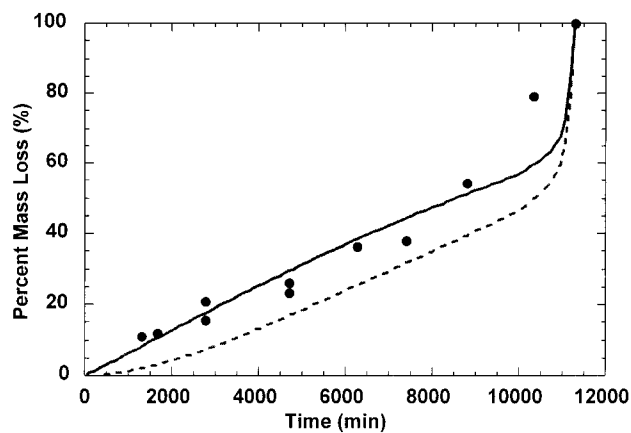


**Figure 4.** Experimental mass loss data for a 4600–5.6 PLA-*b*-PEG-*b*-PLA hydrogel with an average acrylate functionality ( $Z$ ) equal to 0.45 (●). The solid and dashed lines represent the mass loss predictions of the degradation model with (DASHED)  $Z = 1.0$  and (SOLID)  $Z = 0.45$ . Model parameters:  $W_{\text{PEG}} = 0.95, f_c = 0.0, k' = 1.6 \times 10^{-4} \text{ min}^{-1}, X = 1.0$ , and  $L = 25$ .

reacted PLA-*b*-PEG-*b*-PLA segments ( $x_1$ ). Although the mass-loss profiles are similar at early times, the small differences in mass loss prior to reverse gelation result from the relatively more rapid release of singly reacted monomers. In addition, the reverse gelation points differ greatly due to the lowering of the number of cross-links per kinetic chain with an increasing fraction of singly reacted PLA-*b*-PEG-*b*-PLA segments ( $x_1$ ) (see eq 8). This dependence results in shorter degradation times for gels with higher fractions of singly reacted macromer.

For hydrogels with the same degradation rate constant ( $k'$ ), number of cross-links per kinetic chain ( $N$ ), and double bond conversion ( $X$ ), the presence of singly functionalized or singly reacted macromer chain-ends increases mass-loss at early times as shown in Figure 3. This higher percent mass loss occurs due to the accelerated release of the dangling PLA-*b*-PEG-*b*-PLA segments compared to those fully functionalized and doubly reacted. In addition, each of these gels undergoes reverse gelation at the same time (i.e., same extent of degradation) because the number of cross-links per kinetic chain is kept constant by varying the kinetic chain lengths ( $L$ ). Specifically,  $L$  must increase as the degree of double bond functionalization ( $Z$ ) decreases.

The presence of the dangling PLA-*b*-PEG-*b*-PLA segments within the cross-linked network also explains some of the degradation trends observed experimentally. In many cases the original degradation model underpredicted mass loss from the gel at early times ( $P < 0.4$ ).<sup>6</sup> In Figure 4 the experimentally measured mass loss is plotted vs degradation time for a hydrogel formed from a PLA-*b*-PEG-*b*-PLA macromer.

The dashed line represents mass loss predicted by the original model ( $X = 1.0, Z = 1.0$ ), whereas the solid line represents the prediction based on the model incorporating dangling ends ( $X = 1.0, Z = 0.45$ ). Parameters that are common to both models were identical with the assumption of complete acrylate conversion during polymerization. The additional parameter  $Z$  was set to 0.45 based on <sup>1</sup>H NMR characterization of the starting macromer. As shown by the increased overlap with the experimental data, the second model that corrects for the partially reacted macromer segments ( $Z = 0.45$ ) provides a better fit, particularly at early degradation times and also agrees very well with a value of  $Z = 0.40$  determined by applying the method of least squares to the experimental data and model fit.

**Refinement: Multiple Degradable Units.** The derivation of the original degradation model describes the PLA-*b*-PEG-*b*-PLA segments of the hydrogels simply as PEG chains with a single PLA block present on either side. Although each of the two PLA blocks in a macromer is treated distinctly because breaking only one PLA unit has different implications than breaking both, the pseudo first-order hydrolysis kinetics are applied to the entire PLA block, not the individual ester bonds.

To put the variable  $P$  in terms of more useful parameters, the detailed degradation dynamics must be considered. A single PLA block along a PLA-*b*-PEG-*b*-PLA segment is assumed to contain  $j$  number of lactide ester bonds. The number of ester bonds in a single PLA block is important, because if any one of these bonds is hydrolyzed, the cross-link is broken. This identifying characteristic of the network can be used to relate  $P$  to a new probability  $P_E$ , the probability that any random ester bond has been hydrolyzed

$$P = 1 - (1 - P_E)^j \quad (13)$$

Similar to eq 5,  $P_E$  can be written as

$$P_E = 1 - \left( \frac{n_E}{n_E^0} \right) = 1 - e^{-k'_E t} \quad (14)$$

where  $k'_E$  is the pseudo first-order reaction rate constant for the hydrolysis of a single lactide ester linkage. The number of intact ester bonds within the degrading network and the initially undegraded network are represented by  $n_E$  and  $n_E^0$  respectively. Combining eqs 13 and 14 allows one to write  $P$  in terms of  $k'_E$

$$P = 1 - e^{-jk'_E t} \quad (15)$$

Substituting the definition of  $P$  given by eq 15 into the previously developed degradation theory produces a model based on a more fundamental hydrolysis kinetic constant ( $k'_E$ ), which can be verified experimentally and compared to other rate constants reported in the literature. The number of lactide repeat units per PLA block can be verified using  $^1\text{H}$  NMR. PLA-*b*-PEG-*b*-PLA hydrogels with similar swelling characteristics should also produce similar values of  $k'_E$ .

Equation 15 can be rearranged with a knowledge of the triblock cross-link structure to yield a relationship for the cross-linking density of a PLA-*b*-PEG-*b*-PLA hydrogel ( $\rho_C$ ) as a function of degradation time

$$\rho_C \sim (1 - P)^2 \sim e^{-2jk'_E t} \quad (16)$$

A simplified form of the Flory–Rehner equation indicates that the volumetric swelling ratios of these highly swollen, degrading gels are proportional to their cross-linking densities.<sup>13,14</sup> Combining this proportionality with eq 16 leads to the following expression for the swelling ratio of the PLA-*b*-PEG-*b*-PLA hydrogels as a function of degradation time

$$Q \sim \rho_C^{-3/5} \sim e^{6/5jk'_E t} \quad (17)$$

Equations 16 and 17, therefore, predict a dependence of the swelling and overall degradation rate of PLA-*b*-PEG-*b*-PLA hydrogels on the number of lactide linkages present per PLA block. This prediction has been verified through experimental observations. Figure 5 shows the results where  $k'_E$  was determined from the swelling curves of two hydrogels with different numbers of lactides linkages present per PLA block. The macromer used to form hydrogel A contained an average

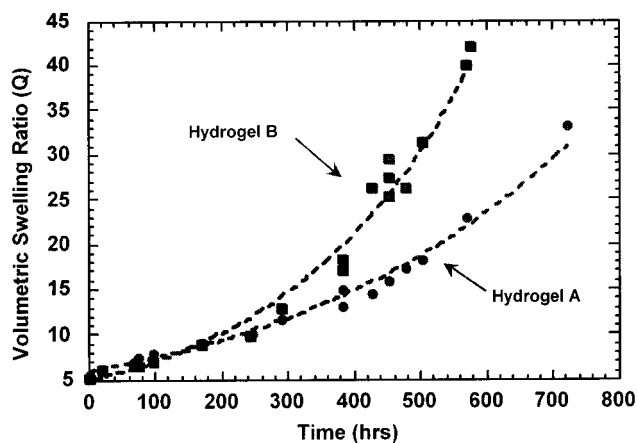


**Figure 5.** Volumetric swelling behavior of two hydrogels polymerized from 20 wt % macromer solutions with different numbers of lactic acid repeat units per PLA block: (**Hydrogel A**)  $2.0 \pm 0.1$  repeat units and (**Hydrogel B**)  $3.3 \pm 0.1$  repeat units. The dashed lines represent the best-fit exponential curves for the data according to the method of least squares and indicate  $k'_E$  values of  $1.6 \pm 0.1 \times 10^{-5} \text{ min}^{-1}$  for the degradation of both hydrogels.

of  $2.0 \pm 0.1$  lactic acid repeat units per PLA block, whereas the macromer of hydrogel B contained an average of  $3.3 \pm 0.1$  lactic acid repeat units in each PLA block (as determined by  $^1\text{H}$  NMR). In the previous modeling approach, fitting the swelling curves to exponential functions would simply generate a different hydrolysis rate constant,  $k'$ , for each gel. However, by normalizing these functions by the number of lactic acid repeat units in each macromer,  $k'_E$  was determined to be identical for both hydrogels ( $k'_E = 1.6 \pm 0.1 \times 10^{-5} \text{ min}^{-1}$ ). This consistent value is expected due to the similar chemistries of the two gels and is comparable to pseudo first-order rate constant values for PLA hydrolysis found in the literature which range from  $1.7 \times 10^{-6} \text{ min}^{-1}$  to  $2.2 \times 10^{-3} \text{ min}^{-1}$ .<sup>15,16</sup>

Comparisons like those presented in Figure 5, based solely on the scaling law given by eq 16, are only valid over small ranges of  $j$ . Large changes in  $j$  affect the cross-linking density, hydrophilicity of the networks, and the amount of water present within the swollen gel. These changes combine to affect the pseudo first-order rate constant  $k'_E$ . Therefore, for gels with substantially different swelling characteristics,  $k'_E$  will vary in a manner that currently can only be explained qualitatively.

**Refinement: Chain-Length Distributions.** The final set of refinements added to the theoretical description for the degradation of these cross-linked networks is the incorporation of a distribution of PLA and/or polyacrylate chain lengths. This addition accounts for both the distribution in the number of repeat units comprising the copolymer cross-links (PLA-*b*-PEG-*b*-PLA segments), as well as the kinetic chains (polyacrylate chains). The distribution of the number of lactic acid repeat units in each PLA block was used to model the macromer chain distribution since this variation is hypothesized to have the greatest effect on degradation behavior. Synthesis conditions of individual macromers, as well as copolymerizations of a variety of macromers, control the final macromer distribution. The distribution of kinetic chain lengths, however, is controlled primarily by polymerization conditions.

*Distribution of Kinetic Chain Lengths.* The original model equations describing the mass loss and bulk degradation of cross-linked hydrogels was applied to a network composed of varying kinetic chain lengths. All PLA-*b*-PEG-*b*-PLA blocks were assigned to a monodisperse distribution to isolate the effects of the kinetic chain length distribution.

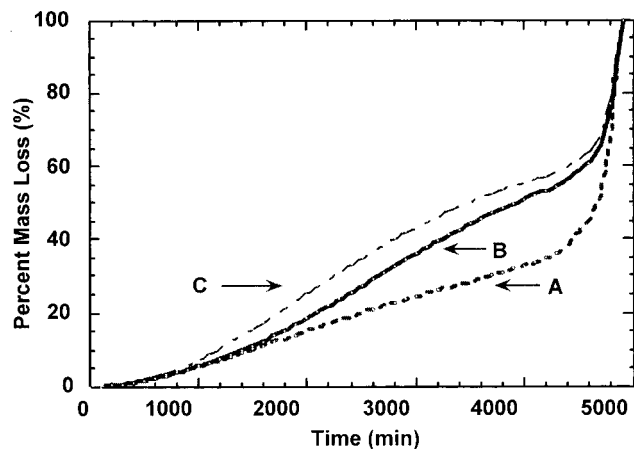


**Figure 6.** Predicted mass-loss behavior from hydrogels with different distributions of kinetic chain lengths: **(Profile A)** monodisperse network with  $L = 100$ ; **(Profile B)** 50/50 bimodal distribution of kinetic chain lengths with  $L_1 = 10$  and  $L_2 = 190$ ; and **(Profile C)** 50/50 bimodal distribution of kinetic chain lengths with  $L_1 = 5$  and  $L_2 = 195$ . Model parameters:  $W_{\text{PEG}} = 0.50$ ,  $f_C = 0.0$ ,  $k'_E = 4.0 \times 10^{-4} \text{ min}^{-1}$ ,  $x_1 = 0.0$ ,  $X = 1.0$ ,  $Z = 1.0$ , and  $j = 1.0$ .

Although the impacts of many kinetic chain length distributions were examined, only a widely spread bimodal distribution with a large network weight fraction of kinetic chains *and* a significant portion of very short kinetic chains had any significant effect on the mass-loss predictions. Figure 6 shows the mass loss predictions of three different hydrogels with different kinetic chain length distributions. All three gels maintain an average kinetic chain length of 100 and therefore undergo reverse gelation at the same time. In profile A, the distribution is monodisperse and all chains contain exactly 100 repeat units. Profile B represents a network with 50% of its kinetic chains only having 10 repeat units, whereas the other 50% have 190 units. Finally, for profile C, 50% of the kinetic chains are only 5 units long and 50% are 195 units long. Only the shorter kinetic chains lead to any significant variation in the mass loss curves. These chains can be released much sooner than longer kinetic chains and, therefore, result in the increased mass loss seen for profile C at early degradation times. With identical values of  $k'$ , all systems undergo reverse gelation at the same time because this event depends only upon the average number of cross-links per chain (Average equals 100 cross-links per chain in all systems). The impact of the kinetic chain length distribution is predicted to be less significant as the weight fraction of kinetic chains in the network ( $W_{\text{PA}}$ ) decreases. Therefore, for experimental PLA-*b*-PEG-*b*-PLA systems with PEG chains larger than 2000 Da (kinetic chains of these systems account for no more than 5% of the network mass), reasonable kinetic chain length distributions are not predicted to have a significant impact on network mass loss.

**Distribution of PLA Block Length.** The mathematical prediction of PLA-*b*-PEG-*b*-PLA hydrogel degradation behavior based on the number and hydrolysis kinetics of individual ester bonds allows quantitative comparison of the degradation behavior of hydrogels made from macromers with varying numbers of lactide units in their PLA blocks. The bulk-degradation model can be further refined to account for variations in the distribution of PLA block sizes within a single hydrogel network. Although the calculations are quite intensive, the degradation behavior of a hydrogel with any chosen statistical distribution of PLA block sizes can be predicted.

In a system with a bimodal distribution of PLA block sizes, there will be PLA blocks with  $x$  number of lactic acid repeat

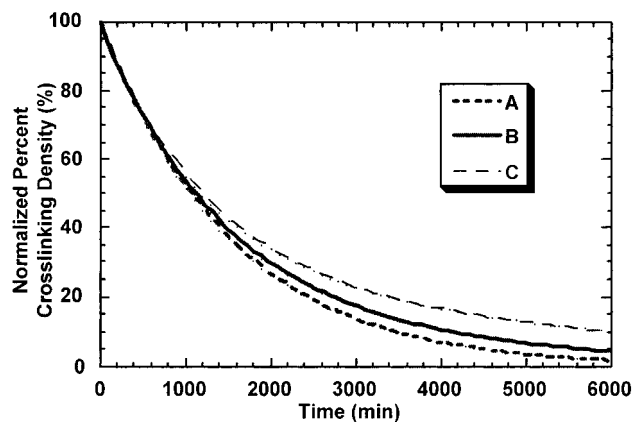


**Figure 7.** Normalized percent cross-linking density as a function of degradation time for hydrogels with increasing polydispersity in their PLA block sizes: **(Curve A)** monodisperse,  $j = 4$ ; **(Curve B)** 50/50 bimodal with  $j_1 = 2$  and  $j_2 = 6$ ; **(Curve C)** 50/50 bimodal with  $j_1 = 1$  and  $j_2 = 7$ . All three systems maintain  $j_{\text{avg}} = 4$ . Model parameters:  $W_{\text{PEG}} = 0.95$ ,  $f_C = 0.0$ ,  $k'_E = 8.3 \times 10^{-5} \text{ min}^{-1}$ ,  $x_1 = 0.0$ ,  $X = 1.0$ , and  $Z = 1.0$ .

units (PLA <sub>$x$</sub> ) and other blocks with  $y$  lactic acid repeat units (PLA <sub>$y$</sub> ). These two distinct blocks can then combine with the PEG chains to form three unique copolymer segments

- (1) PLA <sub>$x$</sub> -PEG-PLA <sub>$x$</sub>
- (2) PLA <sub>$y$</sub> -PEG-PLA <sub>$x$</sub>
- (3) PLA <sub>$y$</sub> -PEG-PLA <sub>$y$</sub>

Similarly, a system with a trimodal distribution of PLA block sizes (PLA <sub>$x$</sub> , PLA <sub>$y$</sub> , and PLA <sub>$z$</sub> ) will form six unique copolymer segments. In addition to the three types listed above, a trimodal PLA system will also contain

- (4) PLA <sub>$x$</sub> -PEG-PLA <sub>$z$</sub>
- (5) PLA <sub>$y$</sub> -PEG-PLA <sub>$z$</sub>
- (6) PLA <sub>$z$</sub> -PEG-PLA <sub>$z$</sub>

No matter what the distribution, each of the triblock copolymer arrangements must be accounted for separately during the bulk degradation of the hydrogel if the mass loss and other macroscopic properties of the degrading gel are to be predicted accurately. Applying a continuous distribution of PLA block sizes, therefore, results in an extremely large number of copolymer combinations and tedious calculations. To simplify these calculations, only bimodal PLA block-size distributions were examined in the current work to illustrate the effect of PLA polydispersity on hydrogel degradation behavior. Such distributions are hypothesized to have the strongest effect on degradation behavior of the gels. In addition, such distributions can also be used to model the hydrogel networks formed by the copolymerization of two or three different degradable macromers.

Figure 7 shows the impact of increasing the dispersity of the PLA oligomeric blocks on the predicted normalized cross-linking density of the hydrogel as a function of degradation time. In curve A, all PLA blocks are monodisperse with four lactic acid repeat units per block. Curves B and C represent bimodal distributions in the PLA block size with 50% of each type (Curve B:  $j_1 = 2$  and  $j_2 = 6$ ; Curve C:  $j_1 = 1$  and  $j_2 = 7$ ). All curves represent hydrogels with an average of four lactic acid

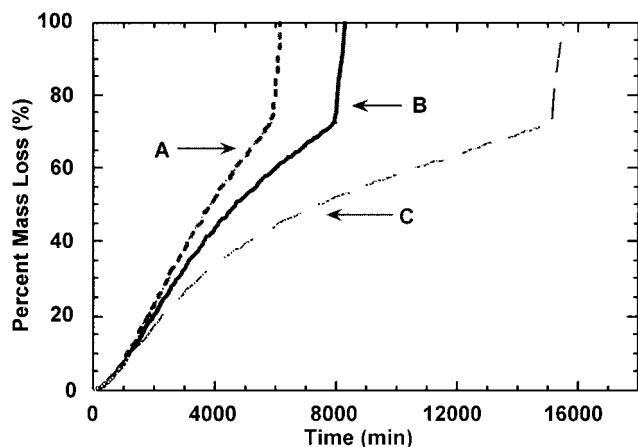


**Figure 8.** Predicted mass loss as a function of degradation time for hydrogels with increasing polydispersity in their PLA block sizes: (Curve A) monodisperse,  $j = 4$ ; (Curve B) 50/50 bimodal with  $j_1 = 2$  and  $j_2 = 6$ ; (Curve C) 50/50 bimodal with  $j_1 = 1$  and  $j_2 = 7$ . All three systems maintain  $j_{\text{avg}} = 4$ . Model parameters:  $W_{\text{PEG}} = 0.95$ ,  $f_c = 0.0$ ,  $k'_E = 8.3 \times 10^{-5} \text{ min}^{-1}$ ,  $x_1 = 0.0$ ,  $X = 1.0$ , and  $Z = 1.0$ .

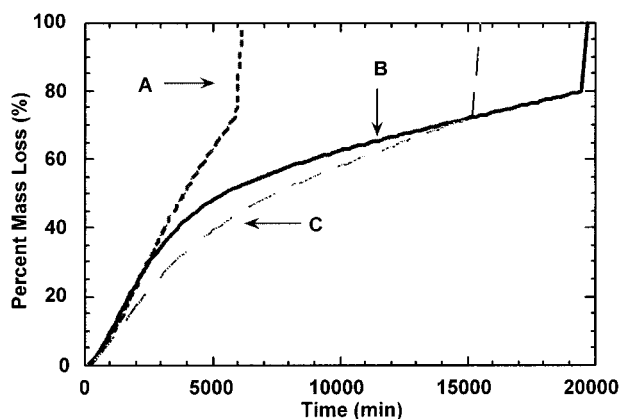


**Figure 9.** Predicted mass loss as a function of degradation time for homogeneously polymerized hydrogels with varying distributions of PLA block sizes and a copolymerized hydrogel: (Curve A) homogeneous, monodisperse,  $j = 4$ ; (Curve B) 50/50 copolymerization of  $j_1 = 1$  and  $j_2 = 7$ ; and (Curve C) homogeneous, 50/50 bimodal with  $j_1 = 1$  and  $j_2 = 7$ . Model parameters:  $W_{\text{PEG}} = 0.95$ ,  $f_c = 0.0$ ,  $k'_E = 8.3 \times 10^{-5} \text{ min}^{-1}$ ,  $x_1 = 0.0$ ,  $X = 1.0$ , and  $Z = 1.0$ .

repeat units per PLA block. Although the average PLA block size is four units in all cases, the normalized cross-linking density increases at any given point in the degradation as one moves from Curve A to Curve C. Thus, with all other conditions being held constant, one would expect a lower swelling ratio, higher compressive modulus, and lower rate of mass loss for hydrogels with increasing dispersion in the degree of polymerization of their PLA blocks.

Figure 8 shows the predicted mass loss profiles for the same three hydrogels as Figure 7. As hypothesized, the hydrogel with the largest distribution of its PLA groups shows the lowest rate of mass loss and the longest time until reverse gelation. This result is very interesting given the fact that all three profiles follow one another until approximately 10% mass loss and only deviate at longer degradation times. Thus, any distribution in the size of the PLA blocks results in a distinctively different mass loss profile that cannot be duplicated simply by changing the degradation rate constant ( $k' = jk'_E$ ) of a monodisperse gel.

Finally, Figure 9 shows the interesting result of using this modeling approach to predict the degradation behavior of a copolymerized, degradable PLA-*b*-PEG-*b*-PLA hydrogel. In this

figure, Curves A and C are the same as in Figure 8 and represent hydrogels with monodisperse ( $j = 4$ ) and bimodal ( $j_1 = 1$  and  $j_2 = 7$ ) distributions within the PLA blocks. Curve B, however, represents the mass loss predicted for a hydrogel constructed from two monodisperse, yet unique, macromers. One macromer has PLA blocks with only 1 lactic acid repeat unit while the other has PLA blocks with only seven lactic acid repeat units. Such a copolymerization produces a different mass-loss curve from the general bimodal distribution because copolymer segments with two different sized PLA blocks (PLA<sub>*y*</sub>-PEG-PLA<sub>*x*</sub>) are not possible. As seen in Figure 9, this type of gel produces a unique mass-loss profile. Although the copolymerized sample initially displays a higher mass-loss rate than the bimodal distribution of Curve C, this gel does not undergo reverse gelation until  $\sim 80\%$  mass loss. These predictions, therefore, indicate that the overall degradation lifetime of a copolymerized gel will be longer than the lifetime of a homopolymerized gel with a similar bimodal PLA distribution.

With the current refinements, the degradation of a homopolymerized PLA-*b*-PEG-*b*-PLA hydrogel can now be predicted accurately using six experimental parameters. These parameters include the following: (1)  $W_{\text{PEG}}$ , the mass percent of the cross-linked network contained in the PLA-*b*-PEG-*b*-PLA segments; (2)  $Z$ , the fraction of macromer chain-ends functionalized; (3)  $X$ , the double bond conversion after polymerization; (4)  $j$ , the number of lactic acid repeat units per PLA segment; (5)  $k'_E$ , the pseudo first-order reaction rate constant for the hydrolysis of a single lactide ester linkage; and (6)  $N$ , the original number of cross-links attached to each kinetic chain. The first four parameters can be determined a priori from characterization of the starting degradable macromer and its polymerization kinetics. A reasonable value for the fifth parameter,  $k'_E$ , can be found in the literature or determined from other macroscopic degradation data such as volumetric swelling ratio or compressive modulus. This analysis only leaves  $N$ , the number of cross-links per kinetic chain, as the only adjustable parameter in predicting the mass loss of these cross-linked hydrogel systems.

## Conclusions

The refinements to a previously developed bulk-degradation model described in this paper were shown to affect different aspects of network degradation to varying extents. The inclusion of partially reacted PLA-*b*-PEG-*b*-PLA segments within the network can have a dramatic effect on the prediction of mass loss and degradation rates. Similarly, characterizing the number of lactic acid repeat units per PLA unit allows the degradation behavior of gels formed from different macromers to be compared quantitatively. Distributions in kinetic chain lengths and PLA segment lengths are also shown to change degradation behavior and can be used to predict the mass-loss profile of copolymerized PLA-*b*-PEG-*b*-PLA hydrogels or hydrogels formed under a variety of polymerization conditions. The common effect is that these refinements describe the cross-linked structure of the PLA-*b*-PEG-*b*-PLA hydrogels more realistically and extend the predictive capability of the original bulk-degradation model.

**Acknowledgment.** The authors thank the National Science Foundation and the Rubber Division of the American Chemical Society for support of this work through fellowships to A.T.M., as well as a grant from the National Institutes of Health (DE 12998).

## References and Notes

- (1) Sawhney, A.; Chandrashekar, P.; Hubbell, J. *Macromolecules*, **1993**, *26*, 581.

- (2) West, J.; Hubbell, J. *Reactive Polymers* **1995**, 25, 139.
- (3) Hill-West, J.; Chowdhury, S.; Sawhney, A.; Pathak, C.; Dunn, R.; Hubbell, J. *Obstet. Gynecol.* **1994**, 83, 59.
- (4) Hill-West, J.; Chowdhury, S.; Slepian, M.; Hubbell, J. *Proc. Natl. Acad. Sci. U.S.A.* **1994**, 13, 5967.
- (5) Elisseeff, J.; Anseth, K.; Sims, D.; et al. *Proc. Natl. Acad. Sci. U.S.A.* **1999**, 96, 3104.
- (6) Metters, A.; Bowman, C.; Anseth, K. *J. Phys. Chem. B* **2000**, 104, 7043.
- (7) Metters, A.; Anseth, K.; Bowman, C. *Polymer* **2000**, 41, 3993.
- (8) Tamada, J.; Langer, R. *Proc. Nat. Acad. Sci. USA* **1993**, 90, 552.
- (9) Amsden, B. *Macromolecules* **1998**, 31, 8382.
- (10) Peppas, N. A.; Ed. *Hydrogels in Medicine and Pharmacy, Vols. 1-3*; CRC Press: Boca Raton, 1986.
- (11) Cukier, R. *Macromolecules* **1984**, 17, 252.
- (12) Metters, A. *Investigation of Degradable, Cross-linked Hydrogels: Prediction of Degradation Behavior*, Ph.D. Thesis, University of Colorado, 2000.
- (13) Flory, P. *Principles in Polymer Chemistry*; Cornell University Press: Ithaca, New York, 1953.
- (14) Metters, A.; Anseth, K.; Bowman, C. *AIChE Journal*, in press.
- (15) Hu, D.; Liu, H. *Polym. Bull.* **1993**, 30, 669.
- (16) Shih, C. J. *Controlled Release* **1995**, 34, 9.